Cosmic Microwave Background Radiation

• CMBR is interpreted as a direct relic of the early (hot) universe.

• It is by far the most **precise** measurement we have in cosmology. (1 part in 10^5).

• Different observational techniques do agree with each other.

There are four basic properties relevant:

▷ Spectrum This results from the conditions during the thermalization epoch ($z = 10^6$ or $t = 1$ year).

▷ Isotropy over large angular scales may be linked to inflation at $z = 10^{27}$ ($t = 10^{-34}$ sec) or earlier.

▷ Distortions from the thermal spectrum, occur because of interactions between thermalization and today.

▷ Anisotropy results from inhomogeneities at decoupling (at the last scattering surface $z = 10^3$ or $t \simeq 10^{5.5}$ years).

CMBR is an isotropic and homogeneous radiation field with a black body spectrum:

$$I_\nu = \frac{2h\nu^3}{c^2}\frac{1}{e^{\frac{h\nu}{kT}} - 1}$$

with $T_0 = 2.726 \pm 0.010^o K$ and $T(z) = T_0\ (1 + z)$.

CMBR

The origin of CMBR is cosmological rather than local because:

• Its energy density $\rho = (\pi^2/15)T^4 = 5 \times 10^{-34}\ gr/cm^3$ or 0.3% of the observable matter today. It is five times the total light density emitted from galaxies, but it is in the microwave region. In view of the above, no obvious local explanation for its existence.

• In order to get that much isotropy from discrete sources a big density of sources is required. The required number is 10^9 times the observed density. Optical depth (due to difusion) is an alternative. To check this, solve 7.1.

• From inverse Compton scattering (Sunyaev-Zeldovich effect) at a $z = 0.54$ cluster of galaxies we deduce that CMBR arrives from earlier in time.

• We also have an atractive theoretical model for its cosmological origin.

Recombination Physics

As the universe expands and cools, there is a time $z_{eq} = 2.3 \times 10^4\ \Omega_0$ when $\rho_{1/3} = \rho_0$. For $z < z_{eq}$ matter density dominates the expansion.

At this time, matter and radiation interact strongly via Thomson scattering ($e\gamma \to e\gamma$). The universe is highly ionized (e,p plus 6% of other elements)

$\Rightarrow$ matter and radiation are in thermal equilibrium.

The temperature must drop well below the ionization threshold of hydrogen (due to the entropy factor = too many photons) in order for matter to combine into electrically neutral atoms.

Due to neutrality, Thomson scattering is supressed and radiation interacts much more weakly with matter

$\Rightarrow$ Matter decouples from radiation.

Matter evolves independently and fluctuations can grow (no stirring due to radiation)

Recombination

The recombination process red

$$p + e \to H + \gamma$$

can be described by the Saha equation.
Ionization fraction: $X = n_e/n_b$ with $n_b = n_p + n_H$.
Use the Boltzman equilibrium distribution for non-relativistic matter (k=1):

$$n = g \int \frac{d^3p}{(2\pi)^3}\, f_B(p) \quad , \quad f_B = \exp[\frac{\mu - E}{T}]$$

with $E = m + \frac{p^2}{2m}$, to obtain

$$n = g\, \left(\frac{mkT}{2\pi}\right)^{3/2}\, \exp[-\frac{m-\mu}{T}]$$

Then $n_H/n_b = 1 - X$, $n_b/n_\gamma = \eta$ and $n_\gamma = 2\zeta(3)T^3/\pi^2$ lead to

$$X = \frac{-1 + \sqrt{1+4S}}{2S} \quad , \quad S = 4\zeta(3)\sqrt{\frac{2}{\pi}}\left(\frac{T}{m_e}\right)^{3/2}\, \eta\; e^{Q/T}$$

with $Q = m_e + m_p - m_H = 13.6\ eV$ and $\zeta(3) \simeq 3.84$.

We can find $X(z)$ by using $T = T_0\ (1+z)$.

Recombination

Asymptotics:

• When $m_e >> T >> Q$,

$S << 1$ and $X \simeq 1$ so the universe is fully ionized.

• When $Q >> T$, $S >> 1$ and $X \simeq 1/\sqrt{S} << 1$ so the universe is neutral.

The transition (recombination) happens at $S \sim 1$.

Puting numbers we find:

$X = 0.9$ at $z = 1450$ and $X = 0.1$ at $z = 1250$,

so $z_{rec} \simeq 1300$ corresponding to

$T = 0.3$ eV, or 3600^o K or

$t_{rec} \simeq 2 \times 10^5$ years

(using $t \simeq 10^{10}(1+z)^{-3/2}$ valid for $z < z_{eq}$.)

The "plasma epoch" where ionized matter dominates the universe spans from

$z_{eq} = 23000\ \Omega_0$ to $z_{rec} = 1300\ \Omega_0$.

Decoupling

After recombination we must find when photons decouple.

As described before we are looking for the freezout point of the Thomson scattering process. This happens when $\Gamma = H$.

Here

$$\Gamma = n_e\ \sigma_T \quad , \quad \sigma_T = \frac{8\pi}{3} r_e^2 = 6.6 \times 10^{-25}\ cm^2$$

and $n_e = X\ n_b = X\ \eta\ n_\gamma$. One obtains $z_{dec} \simeq 1100$ with

$T_{dec} \simeq 0.25$ eV=3000^o K at

$t_{dec} = 3 \times 10^5$ years.

Last scattering surface

After decoupling radiation and matter evolve independently.

Small perturbations in matter can gravitate and grow $\longrightarrow$ structure.

Radiation moves freely carrying the imprint of last interactions.

Look at the photon optical depth (average number of interactions between time t and today) clearly a Poisson process:

$$\tau = \int_t^{t_0} n_e \ \sigma_T \ dt$$

$1 - e^{-\tau}$ is the probability of a photon to be scattered (with change of direction plus loss of coherence).

The visibility function

$$p(z) = \frac{d(1-e^{-\tau})}{dz} = e^{-\tau}\frac{d\tau}{dz}$$

gives the probability that a photon is scatered btween z and $z + dz$.

The last scattering surface is defined by the region in z where the visibility function is substantial.

$p(z)$ turns out to have a Gaussian form with mean value $z_{lss} =$ 1055 and dispersion $\sigma \simeq 75$. Numbers depend on the cosmology but slightly.

$\Rightarrow$ Last scattering surface has finite thickness.

We cannot "see" directly before the last scattering surface due to the "photon fog".

To look earlier we must trace the gravitational or neutrino radiation!

Recombination/Redshift relation

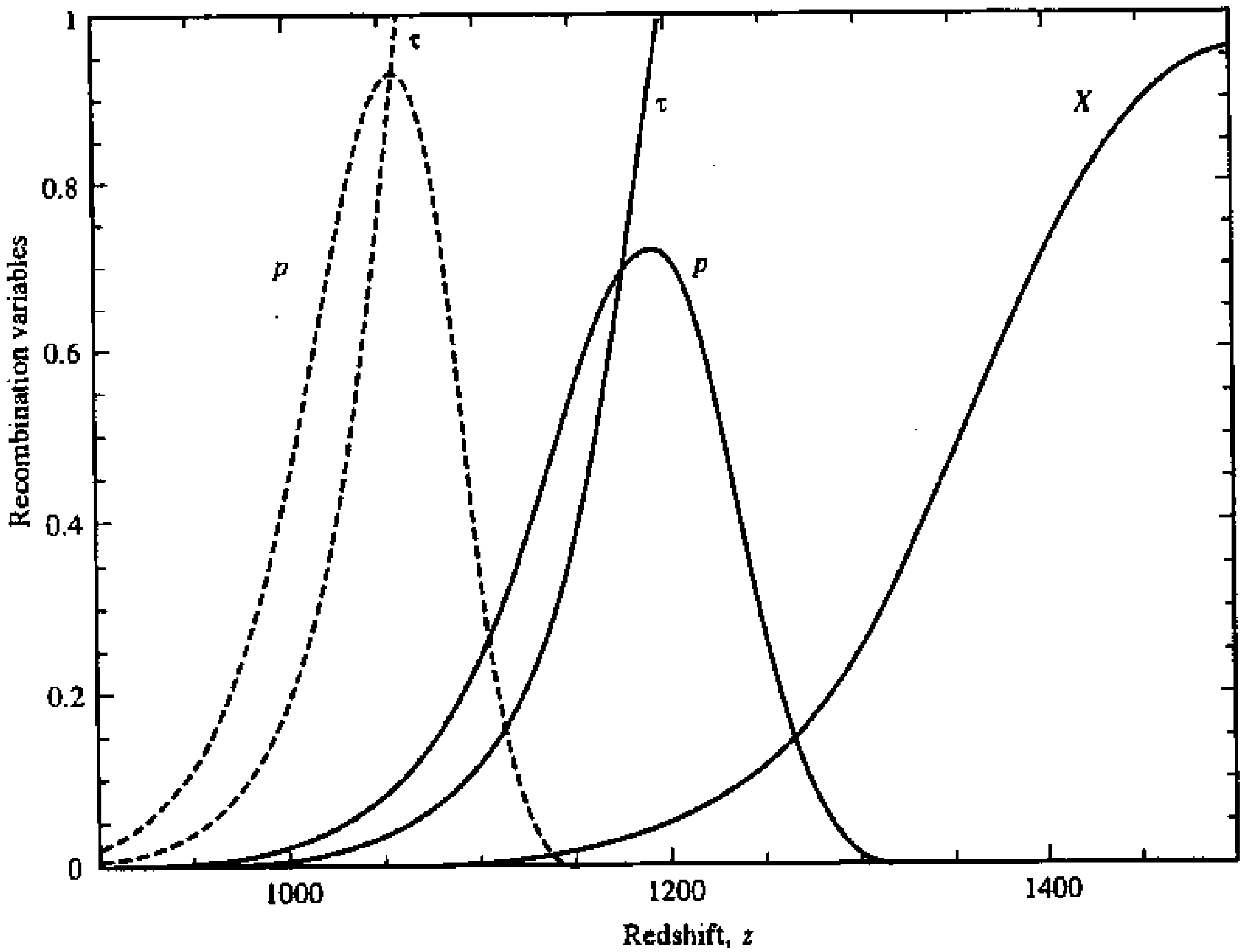

Figure 7.1 Recombination conditions as a function of redshift. The ionization fraction X from the equilibrium (Saha) result (7.3) leads to a recombination redshift $z_{rec} \approx 1300$. The optical depth τ is a sharp function of z with $\tau = 1$ at $z_{lss} \approx 1050$ or 1200 for the dotted line of an $\Omega \ll 1$ universe or the solid line of an $\Omega = 1$ dust universe respectively (both are for $\Omega_b = 0.01$). The last scattering surface is properly given by the visibility function p, with the peak in good agreement with $\tau_{lss} = 1$ and the form fairly Gaussian. A rigorous treatment would include nonequilibrium effects.

Recombination epoch parameters

$z_{eq} = 23000\Omega_0 h^2$	$t_{eq} = \frac{1500}{(\Omega_0 h^2)^{-\frac{3}{2}}}$ y	$T_{eq} = 10$ eV$= 10^5$ K
$z_{rec} = 1300$	$t_{rec} = 2 \times 10^5$ y	$T_{rec} = .3$ eV$= 3600$ K
$z_{dec} = 1100$	$t_{dec} = 3 \times 10^5$ y	$T_{dec} = .25$ eV$= 3000$ K
$z_{lss} = 1055 \pm 75$		

Reionization

It is possible that the universe undergoes a later phase of ionization due to some energy release (galaxy formation etc.)

The last scattering surface will move forward **only if** the optical depth is considerable. For this we need a high reionization fraction and a large path length (given in a matter-dominated universe by $dt \sim (1+z)^{-5/2}dz$)

Assuming $X = 1$ up to z_* we obtain

$$\tau \sim \int n_e dt = \int (1+z)^3 (1+z)^{-5/2} dz \sim (1+z_*)^{3/2}$$

Puting in numbers $\Rightarrow$ lss cannot move unless $z_* > 30$. In that case, CMBR anisotropy can be importantly affected.

Spectrum

At $z = 10^8$ electron-positron anihilation freezes-out.

Dominant processes are photon absortption and emition by charges (thermalization epoch)

These reactions freeze out at $z_{th} \simeq 10^6$ Since then, the spectrum of photons is thermal.

Planck spectrum

$$f = \frac{1}{\exp(h\nu/kT) - 1} \quad ,$$

$$\rho = \frac{\pi^2}{15}T^4 = 4.7 \times 10^{-34}\left(\frac{T}{2.73\ K}\right)^4\ gr/cm^3$$

$$n = \frac{2\zeta(3)}{\pi^2}T^3 = 410\left(\frac{T}{2.73\ K}\right)^3\ cm^{-3}$$

The distribution peaks at $\nu_{max} = 160\left(\frac{T}{2.73\ K}\right)$ GHz or $\lambda_{max} = 1.9\left(\frac{T}{2.73\ K}\right)^{-1}$ nm.

At high frequency we have the Wien limit

$$I_\nu \simeq \frac{2h\nu^3}{c^2}\exp\left[-\frac{h\nu}{kT}\right]$$

while at low frequencies there is the Rayleigh-Jeans region $I_\nu \simeq \frac{2kT\nu^2}{c^2}$

νI_ν is the energy distribution function.

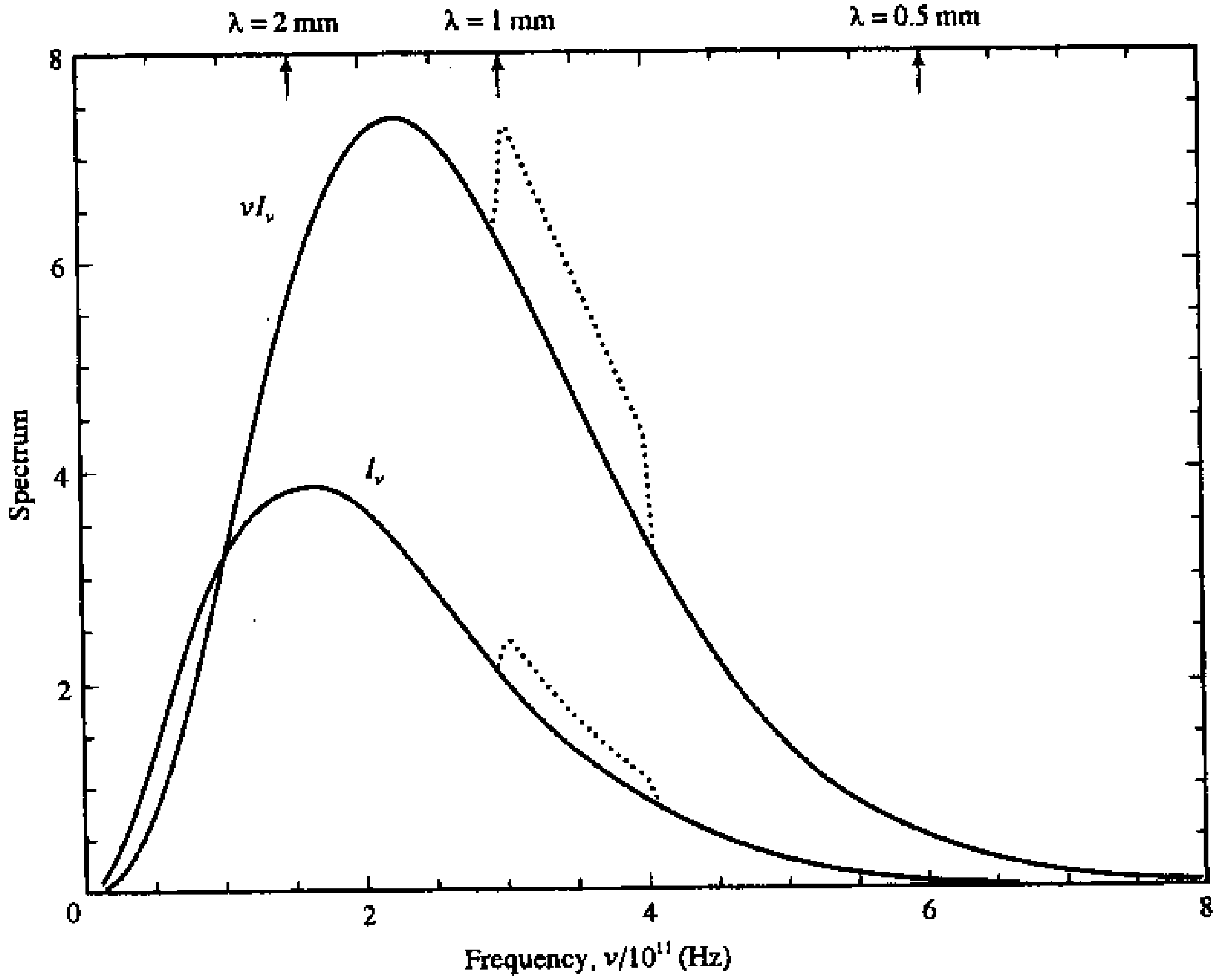

Figure 7.4 The intensity I_ν and energy function νI_ν for a $T = 2.73\,\mathrm{K}$ blackbody, with I_ν in units of $10^{-15}\,\mathrm{erg\,cm^{-2}\,s^{-1}\,Hz^{-1}}$ and the energy function in $10^{-4} c\,\mathrm{erg\,cm^{-3}}$. The dotted bump represents the effect of a deviation between $\nu = 3-4\times10^{11}$ Hz of $\Delta T = +0.1\,\mathrm{K}$. One sees that a relatively modest change in I_ν can be significant when viewed in the physical energy function. At the top are shown the equivalent wavelengths; the CMB peaks at $\lambda = 1.9$ mm.

Measurements

In a typical experimental setup there are

- Frequency-sensitive waveguide
- Reference source for temperature calibration.
- Shielding against ambient heat sources.

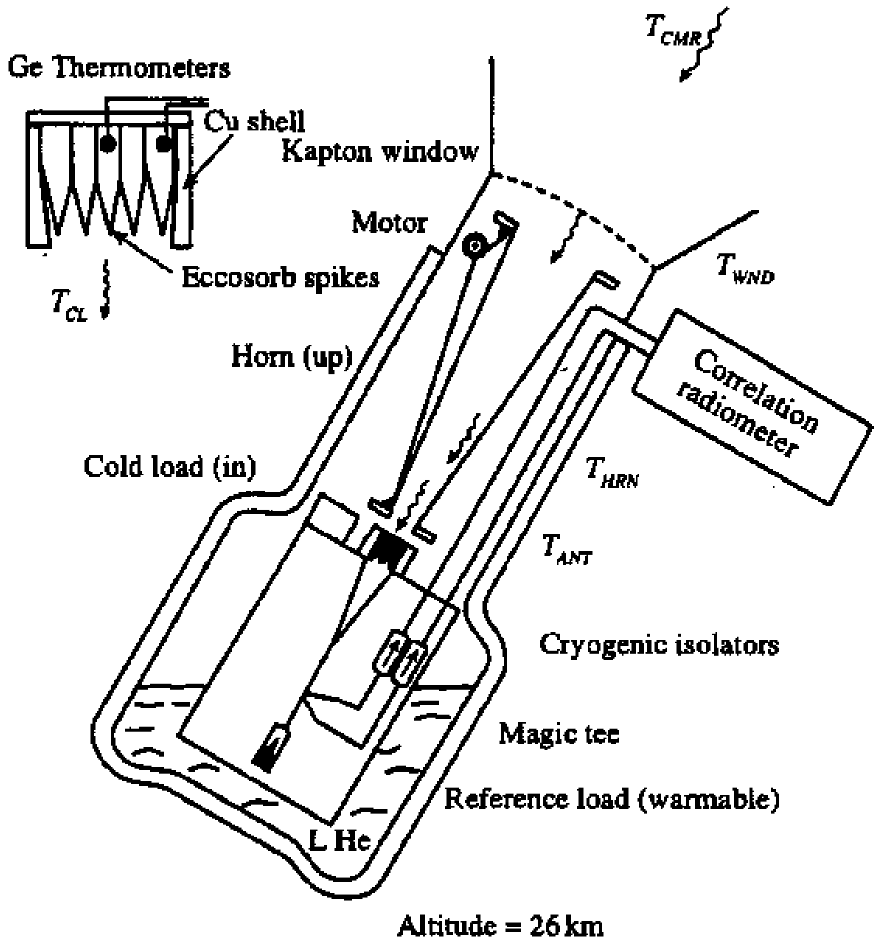

Figure 7.5 Example of an experimental setup for measuring the CMB temperature. (From Staggs, S. and Wilkinson, D. 1991, in *After the First Three Minutes*, eds S.S. Holt *et al.*)

Typical problems arise in the Rayleigh-Jeans region ($\lambda > 30$ cm) due to galactic synchrotron emission and in the Wien region from atmospheric and galactic IR emission.

The techniques: ground-based, balloon-lofted and rocket-flown radiometers, molecular astrophysics and dedicated spacecraft (COBE etc.).

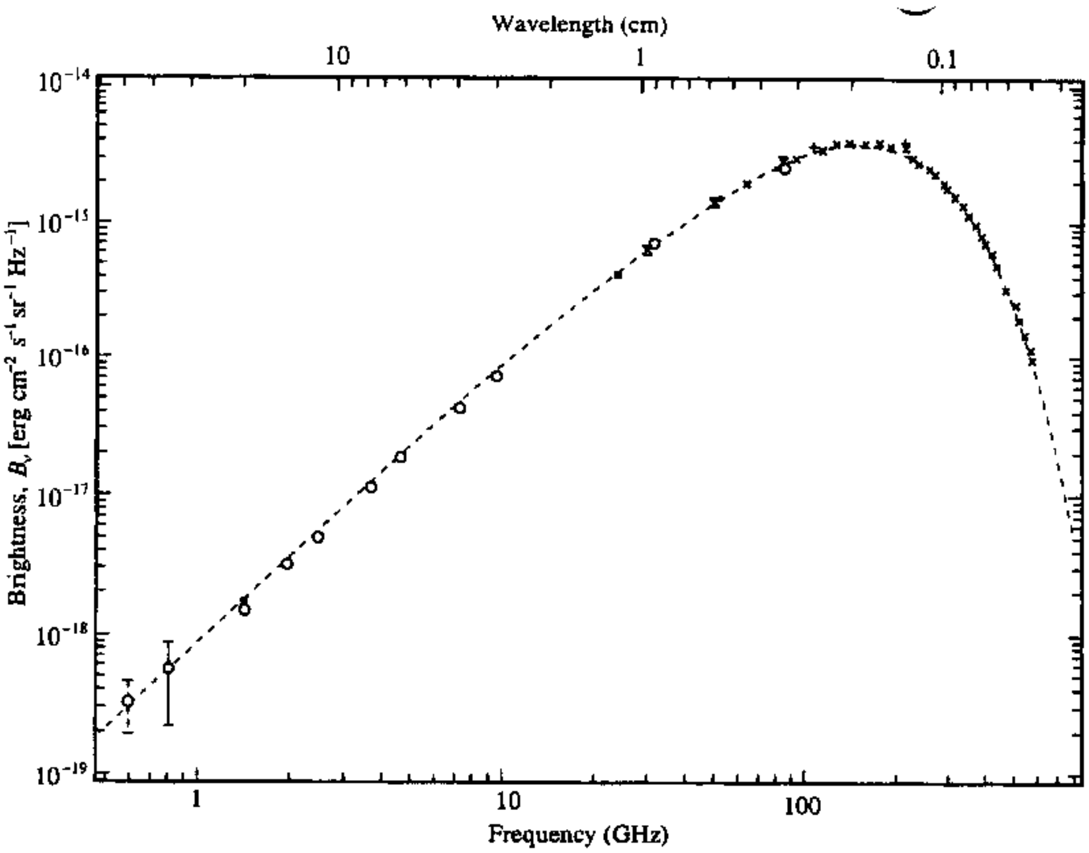

Figure 7.6 Experimental results determining the spectrum of the CMB. Note the excellent agreement with a 2.726 K blackbody (- - -) and the number of different groups and techniques: (●) FIRAS, COBE satellite; (X) DMR, COBE satellite; (○) LBL – Italy, White Mountain and South Pole; (■) Princeton, ground and balloon; (X) UBC, sounding rocket; (+) Cyanogen, optical. From *Cosmology: The Origin and Evolution of Cosmic Structures* by P. Coles and F. Lucchin. © John Wiley & Sons Ltd 1995. Reprinted by permission of John Wiley & Sons Ltd.

Distortions

Interactions after the thermalization epoch $\Rightarrow$ distortions from thermal spectrum.

- Bose-Einstein distortion. Particle interactions generate a chemical potential μ for photons and $\exp[h\nu/kT] \to \exp[(h\nu/kT)+\mu]$. At $\nu \to 0$, $I_\nu \sim \nu^3$.

If energy imput occurs at $z < 4000$ then Compton scattering cannot equilibrate photons. A Compton distortion is produced. COBE puts a limit

$$|\mu| < 3.3 \times 10^{-4}$$

- Atomic transitions can take place during recombination. They would generate a discrete spectrum on top of thermal one.

The dominant lines (Balmer or Lyman) would be redshifter today to $\lambda \simeq 10^{-2}$ cm in the far IR region. This is dominated by galactic emission. In the "visible" radio region only weak transitions (e.g. $16 \to 17$) can occur.

Also, due to last scattering spread, spectral lines are spread ($\Delta\lambda/\lambda \simeq 0.1$ or $\Delta I/I \simeq 5 \times 10^{-6}$), overlap and are dificult to observe.

Distortions

• Comptonization: Later energy releases due to early star formation may reheat the electrons that scatter off photons, redistributiong them in the spectrum. The interaction rate times the average energy shift is given by the Comptonization parameter:

$$y = \sigma_T \int n_e \frac{\Delta\nu}{\nu} dt = \sigma_T \int n_e < v_{||} + v_{||}^2 > dt = \sigma_T \int n_e (T_e/m_e) dt$$

High energy photons are not affected. Low energy photons are redistributed generating an effective temperature:

$$T_{\text{eff}} = T e^{-2y} \quad , \quad \nu_{\text{eff}} = \nu e^{y}$$

COBE limit: $y < 2.5 \times 10^{-5}$

All such distortion mechanisms reprocess photons in other frequency bands.

They are ruled out by observations of the spectrum in multitude frequecies. (COBE at the high end as well as ground-based ones in the low end)

Anisotropy Properties

Relation between angular size of anisotropy and wavelegth of perturbations generating them:

$$\lambda = r_a\ \theta$$

For fluctuations at the last scattering surface:

$$\theta = 1'\left(\frac{\lambda}{h^{-1}Mpc}\right) = 1'\left(\frac{M}{10^{11}h^{-1}M_O}\right)^{1/3}$$

where λ is the present day wavelength and

$$M = \frac{\pi}{6}\rho\lambda^3 = H_0^2\Omega\frac{\lambda^3}{16}$$

is the mass of the corresponding spherical perturbation. The proper size at recombination is λ/z_{rec}. For larger angles $\theta \to 2\sin(\theta/2)$.

Link between CMBR anisotropy and structure formation

There are three angular ranges separated by two special angles:

• The horizon angle $\theta_H \simeq 2^o$ (angular size of the universe at recombination).

• The structure angle $\theta_s \simeq 10'$ corresponds to the scale of fluctuations going non-linear ($\delta\rho/\rho \geq 1$) today.

$\theta_{H,s}$ separate the small angle regime from the medium angle and large angle one.

Anisotropy scales

Regime	Scale	Inducing process
Small angle	$\theta < 10'$	lss,reionization,galaxy, SZ
Medium angle	$10' < \theta < 2^o$	early structure formation
Large angle	$\theta > 2^o$	clustering, voids, SW

Correlation Function

Angular anisotropy: deviation of local temperature $T(\vec{\phi})$ from global mean T.

$$\frac{\Delta T}{T}(\vec{\phi}) \equiv \frac{T(\vec{\phi}) - T}{T}$$

Anisotropy correlation function:

$$C(\theta) = \langle \frac{\Delta T}{T}(\vec{\phi}) \frac{\Delta T}{T}(\vec{\phi}') \rangle_{\theta = |\vec{\phi} = \vec{\phi}'|}$$

θ=dependence only due to homogeneity (no absolute coordinate axes) and isotropy.

$C(\theta)$ is expected to have a maximum at $\theta = 0$ and die-off at large angles. It is also expected to go negative (oscillate) at the wavelegth of relevant perturbations.

This “resonance” is estimated by the coherence angle:

$$\theta_c = \frac{1}{\sqrt{-C''(0)/C(0)}}$$

in analogy with the harmonic oscillator.

Correlations

The first two terms in the correlation function are

$$\frac{C(\theta)}{C(0)} = 1 + \frac{1}{2}\left(\frac{\theta}{\theta_c}\right)^2 + \cdots$$

Flux conservation implies $\int_{\text{sky}} C(\theta) = 0$.

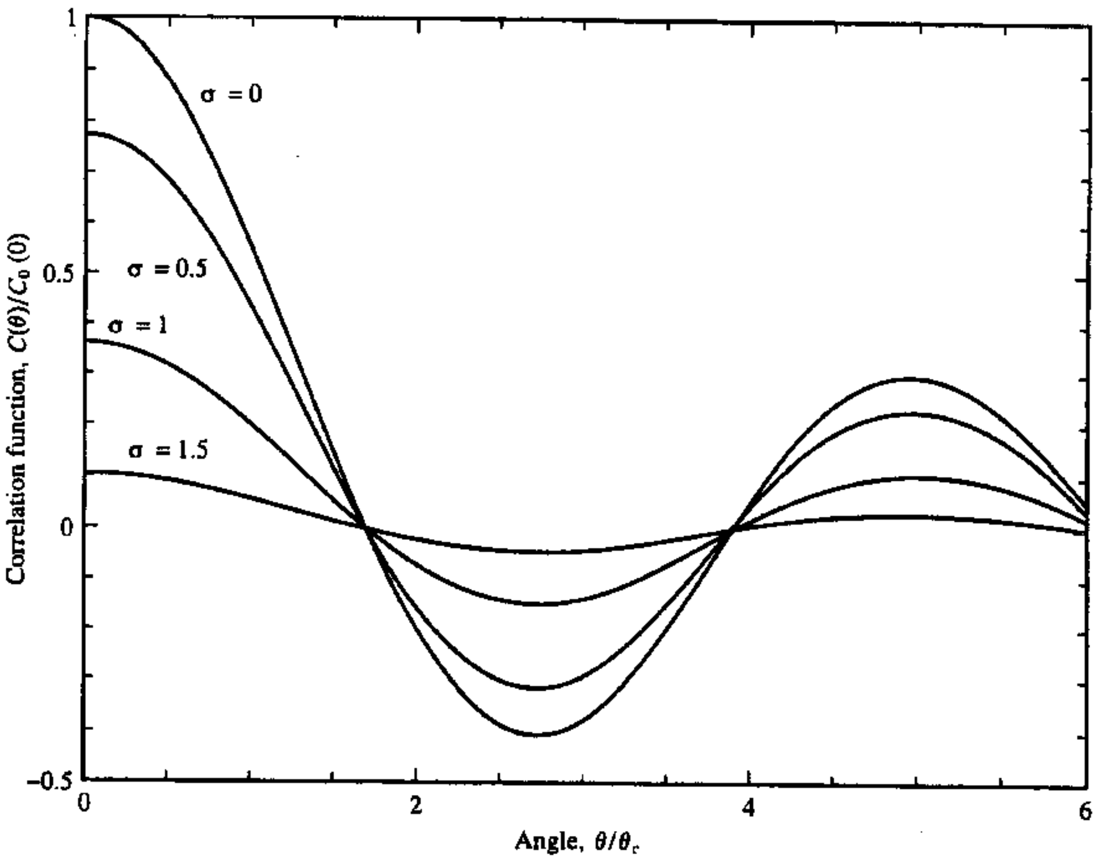

Figure 7.7 Correlation function vs. field separation angle in units of the coherence angle. $C(\theta)$ is modeled by $J_0(\sqrt{2}\theta/\theta_c)$. Also shown are the dilution effects of a Gaussian detector beam smearing with dispersion σ in units of θ_c (see subsection 7.5.4).

Fourier Decomposition

$C(\theta)$ is determined by the underlying fluctuation process.

This becomes visible after Fourier decomposition:

$$\frac{\Delta T}{T}(\vec{\phi}) = \frac{1}{\sqrt{(2\pi)^3}} \int d^3\vec{k}\ h(\vec{k})\ \exp(i\vec{k}\cdot\vec{r})$$

Assuming a power spectrum with

$$\langle h(\vec{k})h(\vec{k}')\rangle = |h(k)|^2 \delta^{(3)}(\vec{k}+\vec{k}')$$

(independent modes) we obtain

$$C(\theta) = \frac{1}{2\pi^2}\int_0^\infty dk\ k^2|h(k)|^2\ \frac{\sin kL\theta}{kL\theta}$$

Assuming Gaussian fluctuations $|h(k)|^2 = \exp[-k^2L^2\theta_c^2/2]$ we obtain

$$C(\theta) \simeq \frac{1}{(\sqrt{\pi}L\theta_c)^3}\exp\left[-\frac{\theta^2}{2\theta_c^2}\right]$$

(validity at small angles).

In order to focus on a specific angular scale, we must decompose into spherical harmonics:

$$C(\theta) = \frac{1}{4\pi}\sum_{l=0}^{\infty}(2l+1)\ C_l\ P_l(\cos\theta)$$

The $l=0$ term corresponds to a monopole, $l=1$ to a dipole, $l=2$ quadrupole etc. A given l term corresponds to $\theta \simeq \pi/l$ for low l and $\theta \simeq 1/l$ for large l.

Thus, θ_H corresponds to $l \simeq 100$ while θ_s corresponds to $l \simeq 400$.

Observations

Experiment measures $C(\theta)$ indirectly.

Typically a double beam at angle θ is used.

Averanging the square of the relative temperature we obtain

$$\left(\frac{\Delta T}{T}\right)^2(\theta) = \frac{\langle[T(\vec{\theta}) - T(\vec{0})]^2\rangle}{\langle T\rangle^2} = 2[C(0) - C(\theta)]$$

In some experiments a three-beam technique is used.

Important factor: beam smearing (reduces resolution)

$$C(\theta) \simeq \frac{1}{(\sqrt{\pi}L\theta_c)^3\Delta}\exp\left[-\frac{\theta^2}{2\theta_c^2\Delta}\right]$$

with $\Delta = 1 + \sigma^2/\theta_c^2$ for a Gaussian beam with dispersion σ.

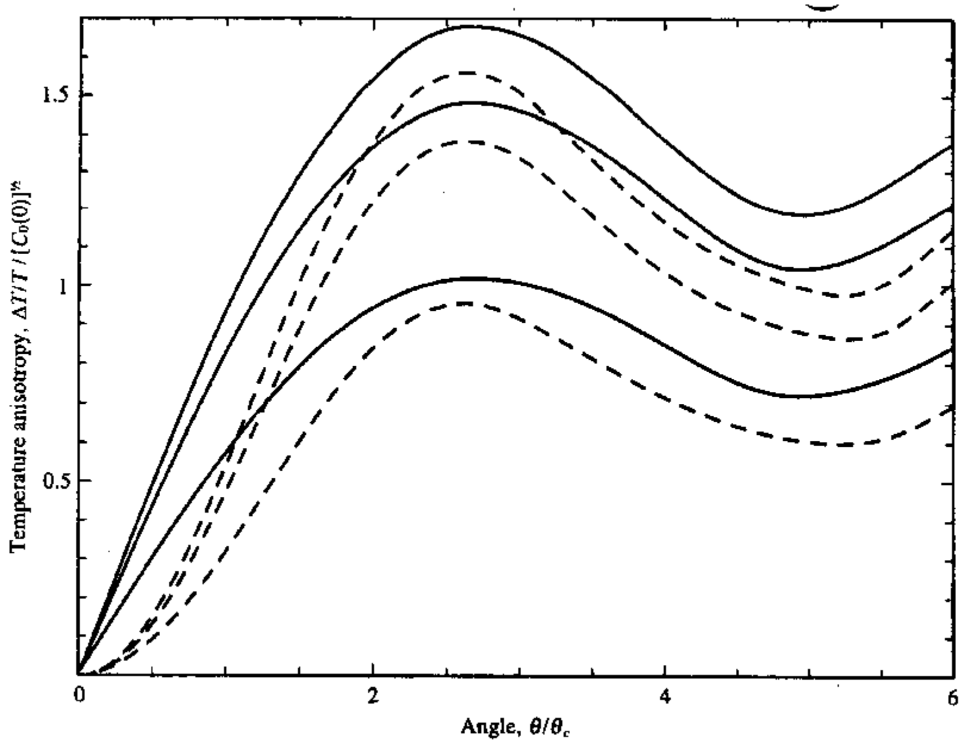

Figure 7.8 The temperature anisotropies corresponding to the correlation function of Figure 7.7. The solid curves are for a two-beam experiment and the dashed curves for a reflected three-beam experiment. The (top, middle, bottom) curve of each set is for beam smearing with $\sigma/\theta_c = (0, 0.5, 1)$.

CMBR Data

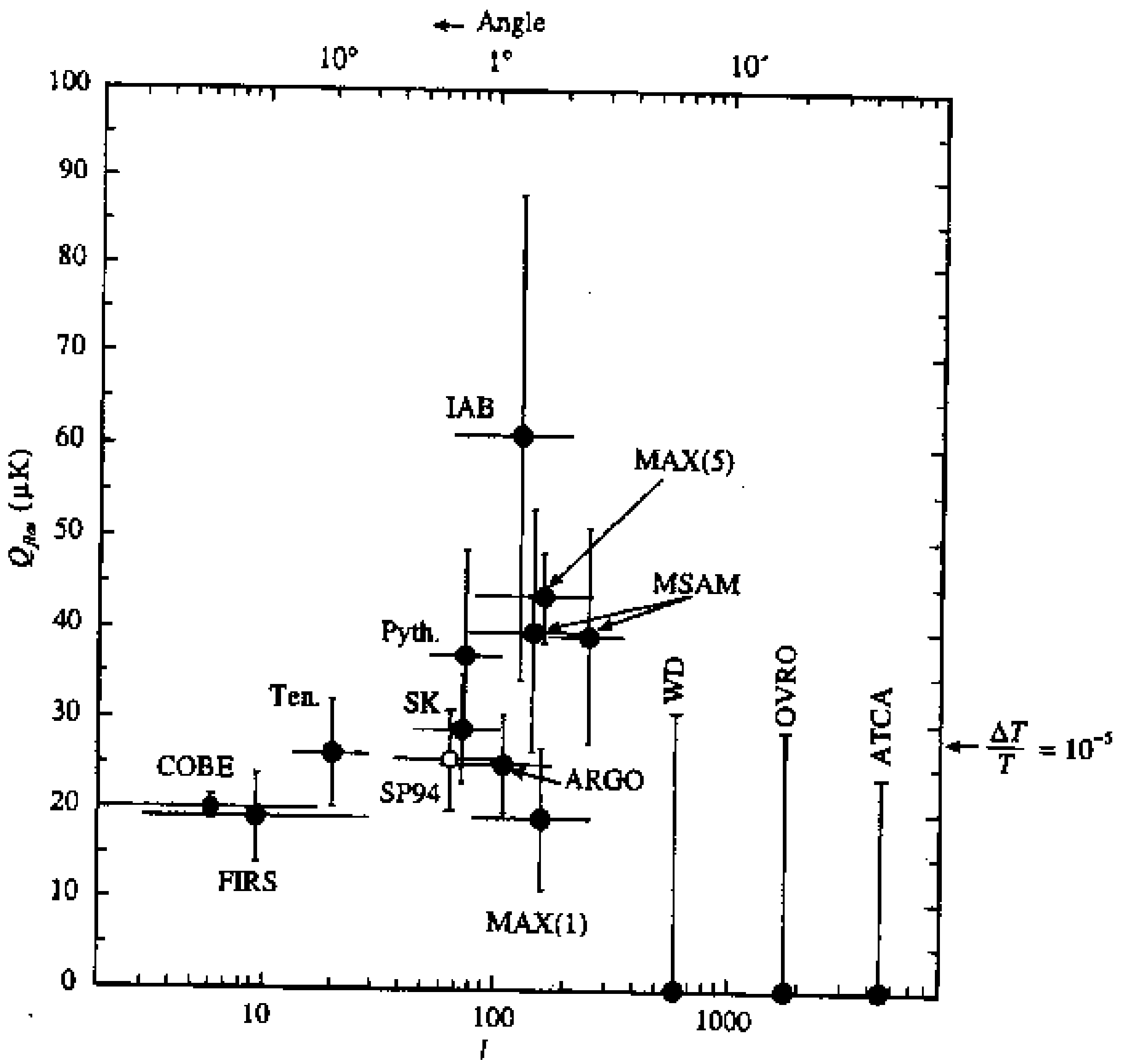

Figure 7.9 Observations and experimental limits on CMB temperature anisotropies on various angular scales. The vertical axis gives the temperature fluctuations measured; 20 μK corresponds to $\Delta T/T = 7 \times 10^{-6}$. The horizontal axis is multipole number or inverse angle; the top axis translates into angle. The horizontal bars on each data point give the angular range of the measurement. Note the number of different groups and techniques. (Reprinted with permission from Silk, J. 1995. *Science* **268**, 829. Copyright 1997 American Association for the Advancement of Science.)

COBE Data

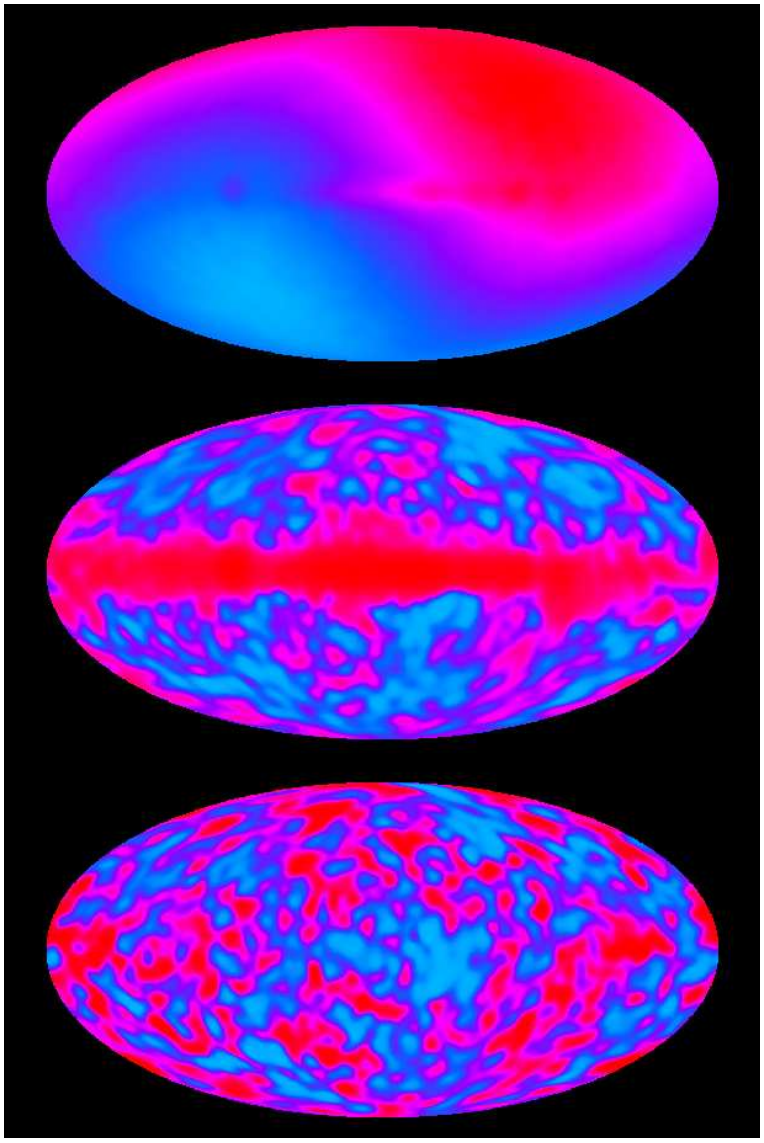

Top: raw data. Middle: dipole subtracted. Bottom: Galactic emission subtracted.

Find more about COBE data at

http://space.gsfc.nasa.gov/astro/cobe/

COBE anisotropy map

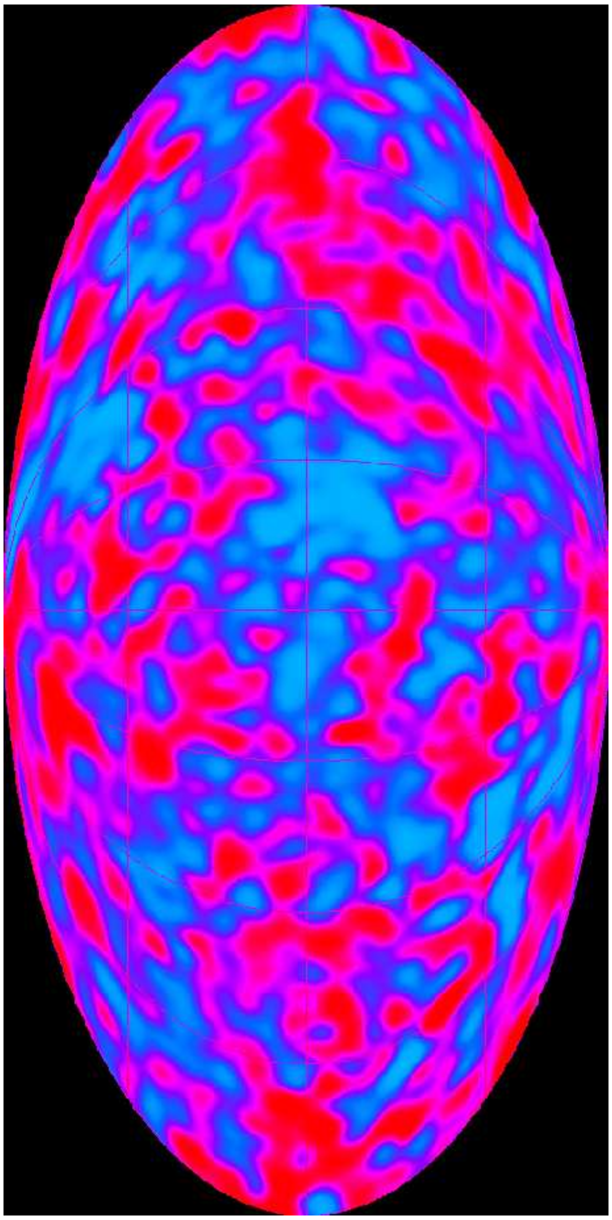

CMBR fluctuations after the subtraction of galactic emission and the dipole

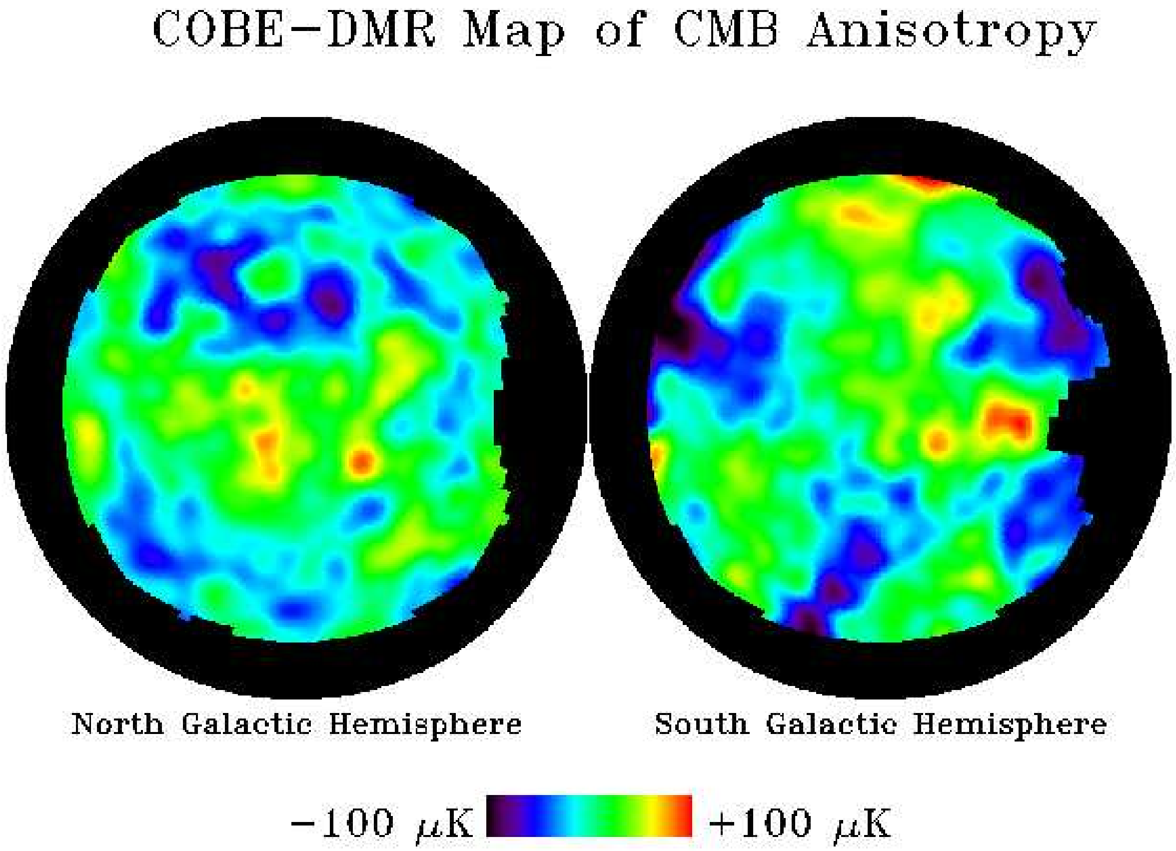
COBE-DMR Map of CMB Anisotropy
North Galactic Hemisphere
South Galactic Hemisphere
−100 μK
+100 μK

Anisotropy Mechanisms

Different physical processes creating anisotropy may have distinguishable signatures:

• Monopole: Incorrect definition of the background temperature.

• Dipole: A Doppler shift due to the source (or observer) motion produces a dipole due to the $\cos\theta$ dependence of $\vec{v}\cdot\hat{n}$.

Earth motion will create a dipole term that needs to be subtracted. This determines

$$v_{\text{galaxy}} = 550\ Km/sec$$

Relativity implies that higher multipoles have also a kinematic component.

Problem: Derive the kinematic quadropole anisotropy.

• Sachs-Wolfe effect: Recent anisotropies tend to have larger λ and smaller r_a thus, larger θ. They come from recent structure formation and fluctuations of gravitational potential. For such angles, recombination details are irrelevant.

At the last scattering surface (lss) $\delta z/z = 150/1050$ so a perturbation with $\lambda > \delta z/z\ r_H \simeq 20 Mpc$ is larger than the thickness of lss. That corresponds to $\theta > 20'$.

Thus large angle predictions are most straightforward, and COBE data are very good.

Anisotropy Mechanisms (Continued)

• Perturbations: Fluctuations at the last scattering surface give rise to anisotropies on medium angular scales. Small perturbations can be decomposed into scalar (density/pressure fluctuations), vector (velocity/rotation) and tensor (gravitational waves) perturbations.

Vector fluctuations damp quickly. Density ones are the most interesting since they give rise to structure formation.

We will show later that because $\Delta n_b/n_b = \Delta n_\gamma/n_\gamma$

$$\frac{\Delta T}{T} = \frac{1}{3}\frac{\Delta\rho}{\rho}$$

To determine the magnitude of anisotropy we must estimate the magnitude of fluctuations.

For a cluster $\Delta\rho/\rho \simeq 2$ and for a galaxy $\Delta\rho/\rho \simeq 10^4$.

To accord with observation we neeed to have structre formation $\Delta\rho/\rho \geq 1$ by $z = 3$. Since (as shown later) $\Delta\rho/\rho \sim 1/a$, it gives a factor of 300 till recombination implying $\Delta T/T \simeq 3 \times 10^{-3}$, a bit too large.

We need to take into account the finite thickness of last scattering surface, and the fact that the primary fluctuations may be in weakly interacting massive particles (WIMPS).

Anisotropy Mechanisms (Continued)

• Sunyaev-Zel'dovich effect: A localized version of Comptonization. As structure forms, the potential energy heats matter. Photons scatter off hot electrons deforming the CMBR.

This effect is the second effect after that dipole that was observed. At cluster positions, anisotropies of 10^{-4} are observed on a $5'$ scale .

• Reionization: It provides a new last scattering surface, rendering recombination effects irrelevant. It wipes out all small scale anisotropies leaving only large scale effects.

It suffers however from (1) dificulties in devising a mechanism that is early without violating COBE data (2) COBE constraints strongly the comptonization parameter, y and (3) Velocity (vector) perturbations arise that give detectble (but not detected) signals.

Thus, today we believe that not much has happpened after recombination.

Constraints for the early universe

CMBR data provide useful constraints for understanding the physics of the early universe.

- Gravitational Waves: The energy density of gravitational waves at cosmological scales ($\lambda > 1$ Mpc) scales as $\Delta T^2/T^2$

For waves generated before recombination we obtain $\Omega_{GW} < 10^{-10}$ while at $z = 3$, $\Omega_{GW} < 10^{-5}$

- Cosmic Strings: These are topological defects that could induce structure formation if their energy density satisfies $G\mu \simeq 10^{-5} - 10^{-6}$.

Straight strings act as gravitational lenses with deflection angle $\delta = 4\pi G\mu$ but also move with $v \simeq 1$. This implies that $\Delta T/T \simeq z \simeq v\delta \simeq 4\pi G\mu$ with a step shift in temperature. Absence of such signatures indicates that $G\mu < 10^{-6}$.

Similar constraints arise from gravitational waves emitted by cosmic strings after recombination (constrained by pulsar timing).

- Inflation: Inflation is associated to an energy scale M_X setting the scale for the false-vaccum energy density. Constraints on gravitational waves and density perturbations during reheating give $M_X < 3 \times 10^{15}$ GeV.

Recent universe constraints

- Cosmic Rays: Although the mean energy of CMBR photons is very low today (around 2.4×10^{-4} eV) they can have important scattering cross sections with ultrafast cosmic rays. For example pion production

$$\gamma + p \to p + \pi^0$$

can occur during collisions with protons with $\gamma = 135MeV/2.4\times$ 10^{-4}eV $.5\times \sim 10^{12}$.

This will cause a cut-off in the cosmic ray energy at 3×10^{20} eV but there are recent vilations of this bound. The reason remains obscure.

- Hubble constant: The Sunyaev-Zel'dovich effect can be exploited: The comptonization parameter $y = \int n_e T_e dt$ is measured for a cluster. The bremsstralung emission $\int n_e^2 T^{1/2} dt$ is also measured.

Hydrostatic equilibrium provides an extra relation between T_e and n_e. From the above $\int dt$ is inferred for the cluster.

If the cluster is assumed spherical this gives a transverse distance which, together with the angular scale of the anisotropy provides an angular diameter distance.

This and a direct measurement of the cluster redshift gives a measurement of the Hubble constant.